PHYSICAL REVIEW C **74**, 051602(R) (2006)

Neutron-to-proton ratios of quasiprojectile and midrapidity emission in the ^{64}Zn + ^{64}Zn reaction at 45 MeV/nucleon

D. Thériault,[1,*] J. Gauthier,[1] F. Grenier,[1] F. Moisan,[1] C. St-Pierre,[1] R. Roy,[1] B. Davin,[2] S. Hudan,[2] T. Paduszynski,[2] R. T. de Souza,[2] E. Bell,[3] J. Garey,[3] J. Iglio,[3] A. L. Keksis,[3] S. Parketon,[3] C. Richers,[3] D. V. Shetty,[3] S. N. Soisson,[3] G. A. Souliotis,[3] B. C. Stein,[3] and S. J. Yennello[3]

[1]*Laboratoire de Physique Nucléaire, Département de Physique, Université Laval, Québec, Québec G1K 7P4, Canada*

[2]*Department of Chemistry and Indiana University Cyclotron Facility, Indiana University, Bloomington, Indiana 47405, USA*

[3]*Cyclotron Institute, Texas A&M University, College Station, Texas 77843, USA*

(Received 26 June 2006; published 27 November 2006)

Simultaneous measurement of both neutrons and charged particles emitted in the reaction ^{64}Zn + ^{64}Zn at 45 MeV/nucleon allows comparison of the neutron to proton ratio at midrapidity with that at projectile rapidity. The evolution of N/Z in both rapidity regimes with increasing centrality is examined. For the completely reconstructed midrapidity material one finds that the neutron to proton ratio is above that of the overall ^{64}Zn + ^{64}Zn system. In contrast, the reconstructed ratio for the quasiprojectile is below that of the overall system. This difference provides the most complete evidence to date of neutron enrichment of midrapidity nuclear matter at the expense of the quasiprojectile.

DOI: 10.1103/PhysRevC.74.051602 PACS number(s): 25.70.Lm, 25.70.Mn

The density dependence of the asymmetry term for nuclear matter is a topic of considerable interest [1,2]. Based on thermodynamic considerations it is possible for the binary nuclear fluid to fractionate into a proton-rich high-density phase and a neutron-rich low-density phase [1]. A manifestation of the density dependence of the asymmetry term from a kinetic perspective would involve the preferential transport of neutrons as compared to protons ("isospin diffusion") when two heavy nuclei collide [3–5]. The overlapping tails of the two colliding nuclei leads to a low-density region into which the preferential flux of neutrons may occur. Neutron enrichment of the low-density phase at midrapidity in comparison to the high-density phase at the projectile and target rapidity might be a result of the density dependence of the asymmetry term. Following the contact phase of the collision, larger surface-to-volume ratio for transiently deformed reaction partners may also result in the preferential emission of neutron-rich clusters in the direction of the contact [6,7]. Experimental results [8–14] show that light particles and fragments emitted at midrapidity exhibit a neutron enrichment compared to the quasiprojectile (QP) or quasitarget (QT) in midperipheral collisions. Results with free-neutron detection aiming to reconstruct completely the midrapidity material (MRM) [15] have been obtained in the reaction ^{129}Xe + ^{nat}Sn at 40 MeV/nucleon. The conclusions of the authors were that, on average, the MRM and the bulk system have an indistinguishable value of their N/Z ratios [15]. In a recent analysis, also with free-neutron detection, results obtained for the reaction ^{58}Ni + ^{58}Ni at 52 MeV/nucleon [16] show that the N/Z ratio of the QP is below the ratio of the initial system and that the MRM ratio could be above the ratio of the initial system. Both experiments used different experimental setups to match neutron and charged-particle data. In the present article, we report on an experimental evaluation of the MRM and QP N/Z ratios made using a single setup, which should allow a more precise measurement of the N/Z ratios.

To examine the potential neutron enrichment of midrapidity nuclear matter we elected to study a symmetric projectile-target system, thus eliminating any initial driving force toward N/Z equilibration. The experiment was performed at the Cyclotron Institute of Texas A&M University, where a ^{64}Zn beam, accelerated to 45 MeV/nucleon, bombarded a self-supporting 5 mg/cm^2 ^{64}Zn target enriched at the level of 99%. Charged reaction products were detected with the FIRST array, consisting of three annular telescopes denoted T1 [270 μm Si(IP)–1 mm Si(IP)–CsI(Tl)/PD], T2 [300 μm Si(IP)–CsI(Tl)/PD], and T3 (300 μm Si(IP)–CsI(Tl)/PD]. These telescopes subtended angles from 2.07° to 27.48° in the laboratory. Isotopic resolution was achieved for ions up to $Z = 12$ in T1, $Z = 8$ in T2, and $Z = 7$ in T3 [17]. Charged particles emitted at larger angles ($36.38° \leqslant \theta_{lab} < 51.11°$) were detected by LASSA telescopes, which provided isotopic resolution for $Z \leqslant 6$ [18]. Charge identification starts at $Z = 3$ for T1, $Z = 2$ for T2, and $Z = 1$ for T3. The electronic trigger required the detection of at least one particle in FIRST. To detect emitted neutrons, seven Bicron BC-501A liquid scintillator cells read out by photomultiplier tubes were mounted outside the scattering chamber at polar angles of 27°, 35°, 50°, 63°, 75°, 105°, and 145°. Neutron energies were determined by time-of-flight measurements and spectra were corrected for background emission using a shadow bar technique. Energetic protons at forward angles were rejected using thin scintillator paddles placed directly in front of the neutron detectors. The neutron efficiency of the experimental setup was determined by using GEANT4 [19] simulations.

We focus on peripheral and midperipheral collisions in which a fragment with $Z \geqslant 9$ and a parallel velocity (beam direction) larger than the center-of-mass velocity (4.5 cm/ns) was detected. The most likely origin of this large atomic

*Corresponding author; E-mail: dany.theriault.1@ulaval.ca

number, Z_{res}, high-velocity fragment is the decay residue of the QP following a noncentral collision. Because of the experimental acceptance the corresponding residue of the QT is not detected. Nevertheless, the symmetry of the system allows us to infer that the average properties of the QP and the QT are the same. In addition, a multiplicity of 4 charged particles and a total detected charge of 25 or more, $Z_{tot} \geqslant 25$ ($Z_{BEAM} = 30$), were also required to ensure sufficient reconstruction of the QP. Nonisotopically resolved ions in FIRST were assigned an average mass based on the initial N/Z of the system for $Z \geqslant 29$ or on the evaporation attractor line [20].

To compare N/Z of the QP to that of the MRM we reconstructed the QP based on the measured residue, bound clusters ($A \geqslant 2$), and free nucleons. For bound clusters, the QP source reconstruction procedure relies on three hypotheses [21]: 1. The heaviest fragment selected as the QP evaporation residue has a velocity close to the QP velocity; 2. the QP emission is isotropic in its reference frame; and 3. all the particles with a parallel velocity greater than that of the residue (forward distribution) were emitted from the QP.

Clusters with a minimum parallel velocity (to minimize the contribution originating from the QT) are attributed to the QP or MRM based on their relative velocity with the QP. For each cluster-QP residue pair, the norm of the relative velocity between a cluster and the residue, V_{rel}, is calculated. The resulting spectra of V_{rel} for hydrogen and helium isotopes with $Z_{res} = 14$ and $Z_{res} = 21$ are displayed in Fig. 1. Evident from these spectra is the fact that backward emission ($V_{rel} < 0$) is favored over forward emission ($V_{rel} > 0$). This result is consistent with previous work [8,22,23]. To facilitate this comparison the distribution for $V_{rel} > 0$ has been reflected, consistent with the isotropic decay hypothesis of the QP. A striking feature of these spectra is that the enhancement of yield for $V_{rel} < 0$ is particularly evident for neutron-rich clusters such as ^{6}He as compared to ^{3}He [9,10]. Deuterons and tritons also exhibit a strong preference for the backward direction. Based upon such experimental V_{rel} spectra, probability tables for attributing a cluster to the QP are constructed. For particles emitted forward of the QP residue the attribution probability is taken to be unity whereas the probability for backward-emitted particles (parallel velocity less than that of the QP residue) the attribution probability is obtained by dividing the forward V_{rel} distribution by the backward distribution. The attribution probability, for each cluster, obtained in this manner depends on both V_{rel} and Z_{res} and is applied on an event-by-event basis. This approach to reconstruct the QP has been previously applied to simulations of the collision (DIT + GEMINI [24,25]) and has been shown to correctly attribute more than 85% of the particles emitted in midperipheral and peripheral collisions [21]. Further details about the reconstruction method and its efficiency are given in Refs. [21,26–28]. Backward-emitted particles that were not assigned to the QP belong to the MRM if their parallel velocity is greater than 2 cm/ns in the reference frame of the QT, which is moving at velocities determined in the proton multisource analysis.

To attribute protons and neutrons to the QP and MRM, the average proton and neutron multiplicities were extracted for three classes of events, namely $Z_{res} = 9$–13, 14–18, and 19–26. It has been previously shown that Z_{res} is correlated

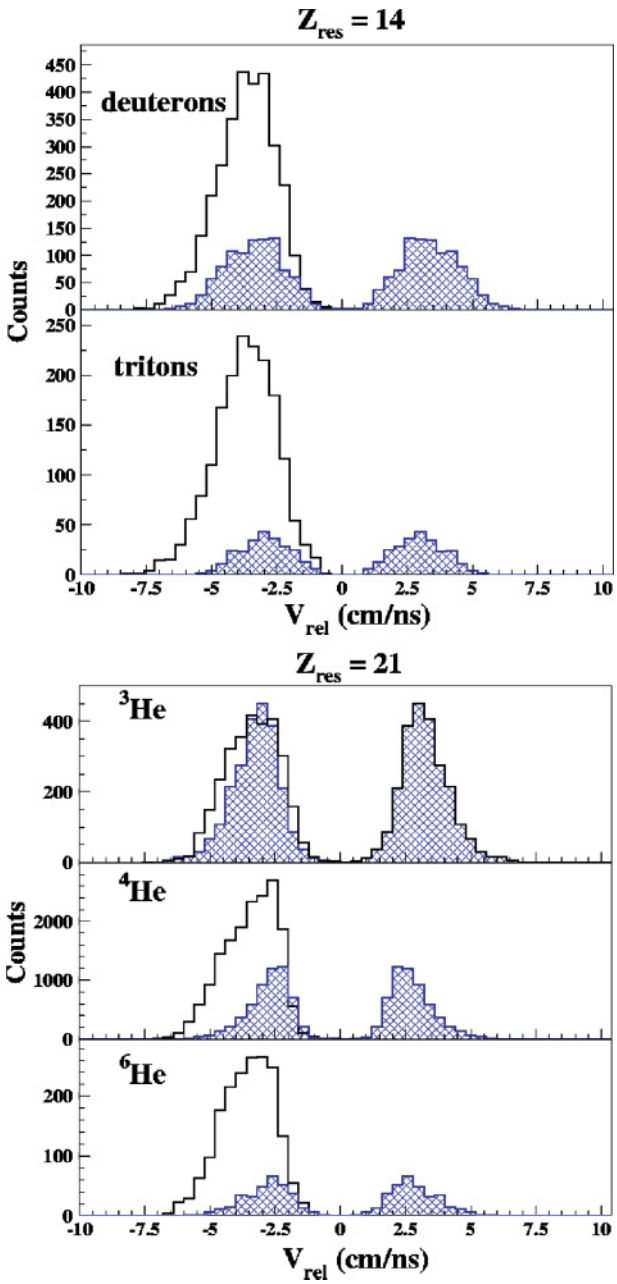

FIG. 1. (Color online) Total relative velocity between a cluster and the QP residue, V_{rel}, backward distribution (clear) and forward V_{rel} distribution backward-reflected (shadowed) for $Z = 1$ isotopes coupled with a QP residue of $Z = 14$ (upper panel) and for $Z = 2$ isotopes coupled with a QP residue of $Z = 21$ (lower panel).

with the excitation energy per nucleon of the QP and is thus a reasonable measure of the centrality of the collision [29,30]. Proton multiplicities are obtained via a moving-source analysis of energy spectra at $\theta_{lab} = 17^{\circ}, 24^{\circ}$, and 43.7° whereas neutron multiplicities were extracted from a moving-source analysis of the background- and efficiency-corrected energy spectra at seven angles. Energy spectra at all angles are fitted simultaneously with the emission from three sources, QP, QT, and a midrapidity "source," although the neutron spectra and proton spectra are treated independently. The midrapidity

source, though perhaps not a single physical statistical source, is necessary to describe the dynamical nucleon emission at midrapidity that contributes to N/Z of the MRM. Each source is characterized by a temperature parameter T, velocity V_s, Coulomb barrier B_c (protons), and a normalization factor N, related to its multiplicity. The nucleon energy (E) distributions are fitted under the assumption of surface emission for the QT and QP sources and volume emission for the MRM by [29–33]

$$\left(\frac{d^2\sigma}{d\Omega dE}\right) = \frac{N}{kT^i}(E - B_c)^j \exp[-(E - B_c)/T], \quad (1)$$

where $(i, j, k) = (2, 1, 4\pi)$ in the case of surface emission and $(i, j, k) = (3/2, 1/2, 2\pi^{3/2})$ in the case of volume emission. Based on the symmetry of the system, it is assumed that QP and QT have the same multiplicity, temperature, and Coulomb barrier whereas the velocity of the MRM is fixed at the nucleon-nucleon center-of-mass velocity (4.5 cm/ns). The spectra associated with the three sources is transformed to the laboratory frame. Figure 2 presents the results of the multisource fits for protons and neutrons at selected centrality classes and angles. As can be seen in these representative spectra the multisource fits provide a reasonably good description of the measured energy spectra. The somewhat poor description of the high-energy tail for the proton spectra at $\theta_{\text{lab}} = 43.7^\circ$ is due to a decreased triggering efficiency for fast protons in the LASSA telescopes. However, the uncertainty associated with the limited experimental data does not significantly affect the multiplicity associated with the QP and MRM. The parameters extracted from the multisource fits are presented in Table I.

In Fig. 3, the dependence of the extracted proton and neutron average multiplicities on the quantity $(Z_{\text{proj}} - Z_{\text{res}})$ is shown. This difference in atomic number is used as a measure of the centrality of the collision, with increasing $(Z_{\text{proj}} - Z_{\text{res}})$ associated with increasing centrality. Evident in Fig. 3 is the slight increase (decrease) of the proton multiplicity for the MRM (QP) with increasing centrality. Measured MRM proton multiplicities are between 1.47 and 1.96 protons/event whereas QP proton multiplicities range from 1.51 to 0.93 protons/event. QP neutron multiplicities are between 0.81 and 0.95 neutron/event and are nearly equal to QP proton multiplicities for the most central collisions studied, a result consistent with the statistical decay of a nearly $N = Z$ QP at high excitation. In contrast, the MRM neutron multiplicity increases from 2.22(±0.27) to 3.25(±0.39) neutrons/event with increasing centrality and is larger than MRM proton multiplicity. The QP is significantly larger in size (see Fig. 4) and presumably at near saturation density. The Coulomb barrier suppresses QP statistical proton emission as compared

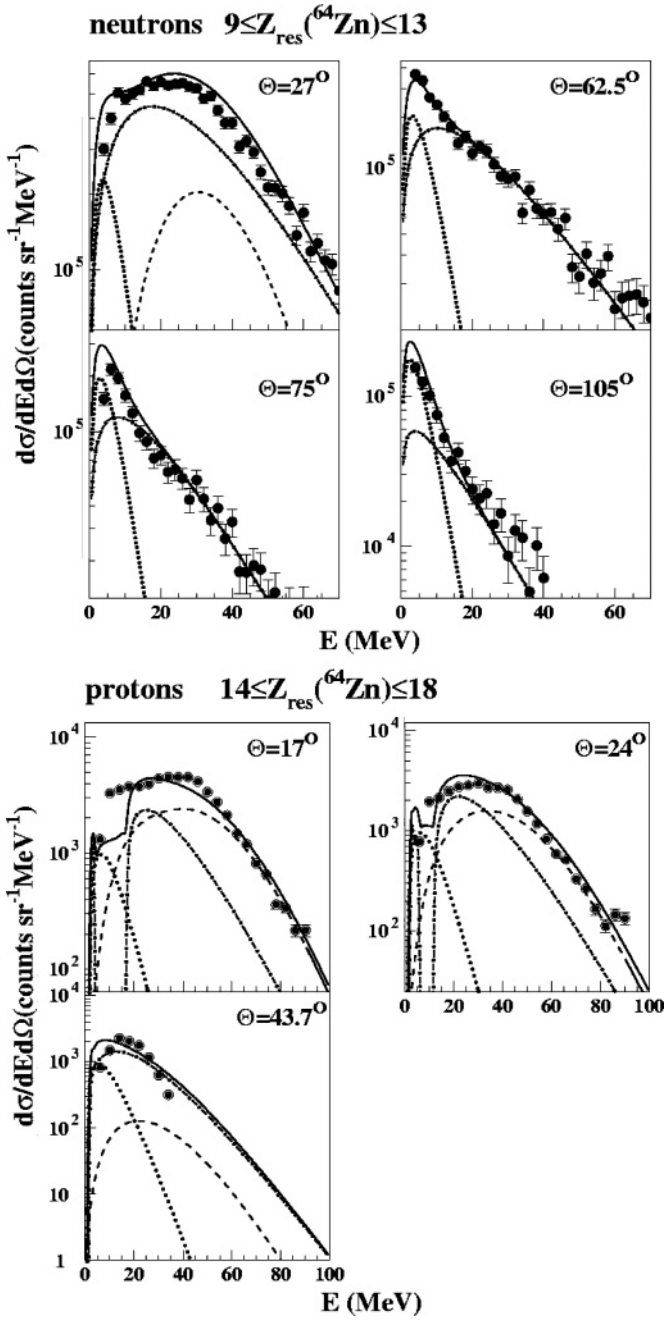

FIG. 2. Multisource fit for free neutrons (upper panel) and free protons (lower panel) at selected angles. Selected centrality classes defined with the charge of the QP residue are shown. QP (dashed lines), QT (dotted lines), MRM (dotted-dashed lines), and total (full lines) contributions are illustrated.

TABLE I. Source parameters extracted from the multisource analysis (with T and B_c in MeV, V in cm/ns, and M in nucleons/event).

Z_{res}	T_{MRM} (n/p)	T_{QP} (n/p)	V_{QP} (n/p)	B_c	M_n (QP/MRM)	M_p (QP/MRM)
9–13	10.9/7.7	2.7/4.3	8.1/7.8	0.06	0.95/3.25	0.93/1.73
14–18	10.7/6.8	2.0/3.7	8.4/8.1	0.38	0.84/2.95	1.01/1.96
19–26	10.5/6.5	2.2/2.7	8.4/8.4	1.00	0.81/2.22	1.51/1.47

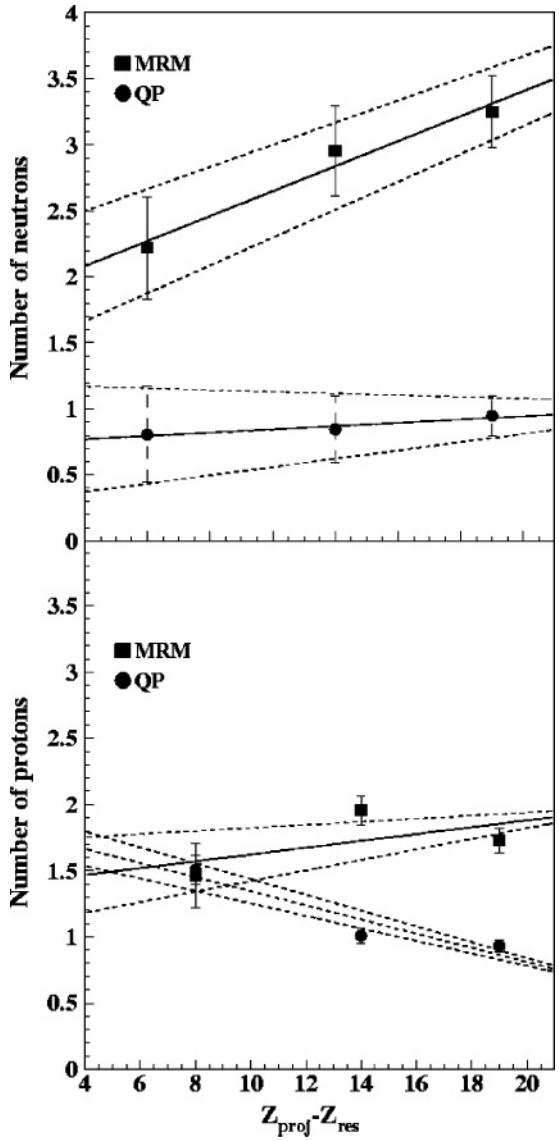

FIG. 3. Free-neutron (upper panel) and proton (lower panel) average multiplicities as a function of the projectile charge minus the average QP residue charge. QP (dots) and MRM (squares) multiplicities are illustrated. Solid lines are fitted to the obtained values and dashed lines to the upper and lower uncertainties.

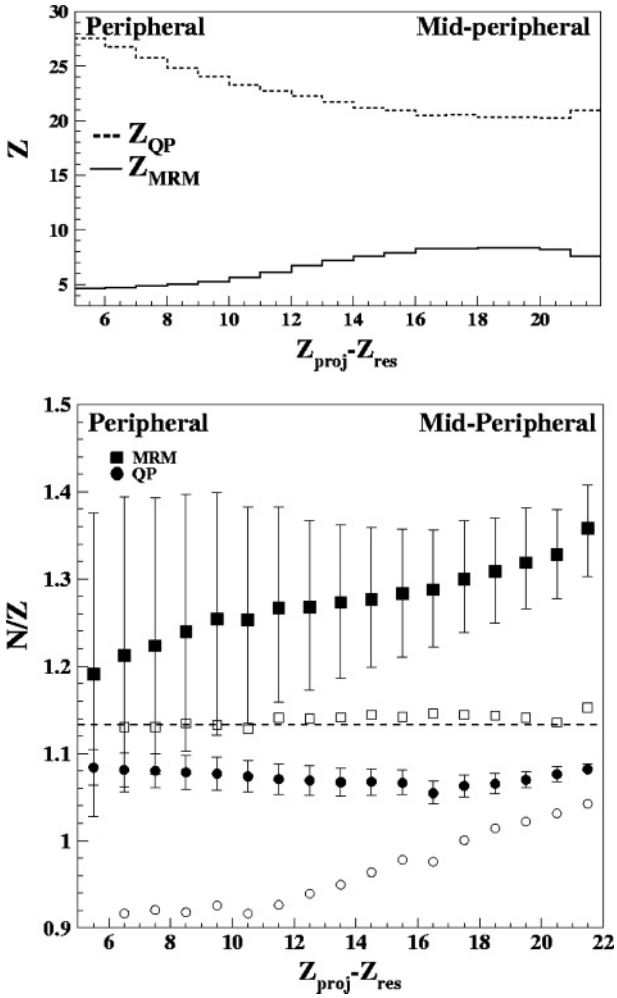

FIG. 4. Upper panel: Average charge of the QP and MRM as a function of the charge difference between the projectile and the residue. Lower panel: Average N/Z ratios of QP (solid circles) and MRM (solid squares) as a function of the charge difference between the projectile and the residue. The open symbols correspond to the clusters. Thin dotted line: original N/Z of the projectile and target. Errors reported reflect the multisource fit uncertainty for free nucleons.

to QP neutron emission. Nevertheless, the neutron multiplicity extracted for the MRM is two to three times larger than for the one associated with the QP. The extracted multiplicities were linearized, as shown in Fig. 3, to provide a continuous relation between the multiplicities of free nucleons and centrality. Error bars extracted from the optimization are shown.

Evident in the top panel of Fig. 4 is the dependence of the atomic number of the reconstructed QP and MRM (free nucleons, particles, and all heavier fragments) on centrality. With increasing centrality the size of the QP decreases from $Z \approx 28$ to $Z \approx 21$ whereas the size of the MRM increases from a value of $Z \approx 5$ to $Z \approx 8$. The decrease in the size of the QP is associated with an increase in the emitted charge. For peripheral collisions, $Z_{\mathrm{res}} = 25$ and $Z_{\mathrm{emitted}} = 3$ but for midperipheral collisions $Z_{\mathrm{res}} = 9$ and $Z_{\mathrm{emitted}} = 12$, consistent with increased excitation. For the most central collisions presented, the atomic number of the QP and MRM are constant.

The average N/Z of the reconstructed QP and MRM (free nucleons, particles, and all heavier fragments) are displayed in the lower panel of Fig. 4. A clusterized charge of at least 2 units is required in the MRM to avoid MRM N/Z ratios computed only with free nucleons. The value of the N/Z ratio for the MRM (solid squares) increases with increasing centrality from 1.19 (peripheral) to 1.35 (semiperipheral). For reference, N/Z of the system (1.13) is indicated as the dashed line. Over the entire centrality range examined, N/Z of the MRM exceeds N/Z of the system. In contrast, N/Z of the QP (solid circles) is relatively constant over the same centrality range with a value of $\approx 1.07 \pm 0.04$, slightly less than the N/Z ratio of the original system. The uncertainty in the reconstructed N/Z lies largely with the uncertainty in the nucleon emission. To assess

this uncertainty we used extreme assumptions regarding the contribution of free-nucleon emission to N/Z of the QP and MRM consistent with the measured multiplicities displayed in Fig. 3. The maximum (minimum) neutron multiplicity possible for a particular centrality was assumed to be associated with the minimum (maximum) proton multiplicity resulting in the largest (smallest) N/Z. The uncertainties displayed therefore correspond to the maximum uncertainties on N/Z from the free-nucleon multiplicities. Despite the large uncertainties associated with N/Z for the MRM, for midperipheral collisions, a clear neutron enrichment is observed at the expense of the QP. In addition to the uncertainty associated with the free-nucleon multiplicities, tests were conducted to evaluate the uncertainty associated with the minimal clusterized charge required in the MRM, the mass of the nonisotopically resolved fragments, and also the Coulomb influence of the target on the particles with differing N/Z. In all these tests, a neutron enrichment of the MRM is observed and the calculated MRM N/Z is between 1.29 and 1.37 for the most central collisions studied here.

To understand the observed trends in N/Z for the QP and MRM, we have further examined N/Z associated with clusters ($A \geqslant 2$). In the case of the MRM (open squares), N/Z is constant with centrality and has a value close to that of N/Z of the system. In contrast, for the case of the QP (open circles), where we additionally exclude the QP residue from the calculation of N/Z, a centrality dependence is observed. Although for the most peripheral collisions, N/Z of the clusters attributed to the QP is approximately 0.9, with increasing centrality this value increases toward 1.05. These observed trends in N/Z associated with clusters can be understood quite simply. In the case of the MRM, the tendency to clusterize at low density is strongly driven by α-particle formation and to a lesser extent deuteron formation. Formation of these $N = Z$ clusters dominates all other clusters. Formation of other neutron-rich clusters, such as tritons and ^{6}He, explains why the average value of N/Z is larger than unity. Examples of the relative yield of these light clusters is apparent in Fig. 1. In the case of the QP, the measured N/Z associated with clusters is primarily driven by the ratio of ^{3}He and ^{4}He at low excitation and the emission of heavier neutron-rich clusters with increasing excitation.

Consequently, the increase in N/Z for the MRM stems largely from the preferential free neutrons as compared to free protons and clusters in this regime. One can therefore conclude from Fig. 4 that, on average, the QP, and presumably the QT, preferentially transfer neutrons to the MRM. This transfer is around 0.3 to 1.7 neutrons for the present reconstruction, as deduced from Fig. 4. Although the small number of neutrons transferred does not change the QP N/Z significantly because of its large size ($21 \leqslant \langle Z_{\mathrm{QP}} \rangle \leqslant 28$), it is a significant change for the much smaller MRM ($5 \leqslant \langle Z_{\mathrm{MRM}} \rangle \leqslant 8$). For the presently studied symmetric system, the Coulomb push of emitted particles by the QP and QT should be roughly equal at midrapidity, thus contributing negligibly to a systematic suppression of neutron-rich clusters in the MRM. Neutron-skin effects, for elements of the size of the ^{64}Zn, should also be negligible [34].

In summary, we observed that the average N/Z ratio of MRM is above the N/Z ratio of the original system for midperipheral reactions of the $^{64}\mathrm{Zn} + {}^{64}\mathrm{Zn}$ system at 45 MeV/nucleon. This neutron enrichment of midrapidity nuclear material is at the expense of the QP, which systematically has a N/Z ratio below that of the system. A likely origin for the preferential transfer of neutrons toward midrapidity is a density dependence of the symmetry energy [35,36].

This work was supported in part by the Natural Sciences and Engineering Research Council of Canada, the Fonds pour la Formation de Chercheurs et l'Aide à la Recherche du Québec, the U.S. Department of Energy through Grant Nos. DE-FG-92ER40714 (IU) and DE-FG03-93ER40773 (TAMU), and the Robert A. Welch Foundation through Grant No. A-1266.

[1] H. Müller and B. D. Serot. Phys. Rev. C **52**, 2072 (1995).
[2] *Isospin Physics in Heavy-Ion Collisions at Intermediate Energies*, edited by W. Udo Schröder and B. Li, (Nova Science Publishers, New York, 2001).
[3] L. Shi and P. Danielewicz. Phys. Rev. C **68**, 064604 (2003).
[4] B.-A. Li, Phys. Rev. C **69**, 034614 (2004).
[5] V. Baran *et al*., Phys. Rev. C **72**, 064620 (2005).
[6] S. Hudan *et al*., Phys. Rev. C **70**, 031601(R) (2004).
[7] S. Hudan R. T. de Souza, and A. Ono, Phys. Rev. C **73**, 054602 (2006).
[8] E. Plagnol *et al*., Phys. Rev. C **61**, 014606 (1999).
[9] J. F. Dempsey *et al*., Phys. Rev. C **54**, 1710 (1996).
[10] S. Hudan *et al*., Phys. Rev. C **71**, 054604 (2005).
[11] Y. Larochelle *et al*., Phys. Rev. C **62**, 051602(R) (2000).
[12] P. M. Milazzo *et al*., Phys. Lett. **B509**, 204 (2001).
[13] D. Shetty *et al*., Phys. Rev. C **68**, 054605 (2003).
[14] L. G. Sobotka, J. F. Dempsey, R. J. Charity, and P. Danielewicz, Phys. Rev. C **55**, 2109 (1997).
[15] L. G. Sobotka *et al*., Phys. Rev. C **62**, 031603(R) (2000).
[16] D. Thériault *et al*., Phys. Rev. C **71**, 014610 (2005).
[17] T. Paduszynski *et al*., Nucl. Instrum. Methods A **547**, 464 (2005).
[18] B. Davin *et al*., Nucl. Instrum. Methods A **473**, 302 (2001).
[19] S. Agostinelli *et al*., Nucl. Instrum. Methods A **506**, 250 (2003).
[20] R. J. Charity, Phys. Rev. C **58**, 1073 (1998).
[21] L. Gingras *et al*., *Proceedings of the XXXVI International Winter Meeting on Nuclear Physics*, Bormio, Italy, January 25th–31st, edited by I. Iori, Dept. of Physics, University of Milano, p. 365, 1998.
[22] C. P. Montoya *et al*. Phys. Rev. Lett. **73**, 3070 (1994).
[23] T. Lefort *et al*., Nucl. Phys. **A662**, 397 (2000).
[24] R. J. Charity *et al*., Nucl. Phys. **A483**, 371 (1988).
[25] L. Tassan-Got and C. Stéphan, Nucl. Phys. **A524**, 121 (1991).
[26] Z. He *et al*., Phys. Rev. C **63**, 011601(R) (2000).
[27] L. Gingras *et al*., Phys. Rev. C **65**, 061604(R) (2002).
[28] Z. He *et al*., Phys. Rev. C **65**, 014606 (2002).
[29] D. Doré, Phys. Lett. **B491**, 15 (2000).
[30] G. Lanzano *et al*., Nucl. Phys. **A683**, 566 (2001).
[31] A. S. Goldhaber, Phys. Rev. C **17**, 2243 (1978).
[32] R. Wada *et al*., Phys. Rev. C **39**, 497 (1989).
[33] Y. Larochelle *et al*., Phys. Rev. C **59**, R565 (1999).
[34] L. G. Sobotka, Acta Phys. Pol. B **31**, 1535 (2000).
[35] V. Baran *et al*., Nucl. Phys. **A632**, 287 (1998).
[36] Y. Zhang and Z. Li, Phys. Rev. C **71**, 024604 (2005).